

Bound states in waveguides and bent quantum wires. I. Applications to waveguide systems

John P. Carini

Department of Physics, Indiana University, Bloomington, Indiana 47405

J. T. Londergan

*Department of Physics, Indiana University, Bloomington, Indiana 47405
and Nuclear Theory Center, Indiana University, 2401 Milo Sampson Lane,
Bloomington, Indiana 47408-0768*

D. P. Murdock

*Nuclear Theory Center, Indiana University, 2401 Milo Sampson Lane, Bloomington, Indiana 47408-0768
and Department of Physics, Tennessee Technological University, Cookeville, Tennessee 38505*

Dallas Trinkle

Department of Physics, Xavier University, Cincinnati, Ohio 45207

C. S. Yung

Department of Physics, Texas A&M University, College Station, Texas 77843

(Received 5 August 1996)

It has been shown that in quantum wires which contain bends there will be one or more bound states for electrons placed in such systems. Bound states have been observed in quantum wires, but detailed mapping of such states is difficult. However, there is a one-to-one correspondence between wave functions of free electrons in two-dimensional (2D) systems, and electric fields of TE modes in rectangular waveguides with the same cross section as the 2D system. We therefore construct bent waveguides, find the frequencies at which confined EM fields occur, and map out the electromagnetic energy density there. We compare the experimental results with theoretical predictions of bound state energies and eigenfunctions. The geometry has been chosen to correspond to two-dimensional systems for which quantum wire experiments have been carried out. In such systems, we can predict the number and location of the bound states in the system; in addition, we can predict the electric and magnetic fields for the confined TE modes in this system. We show very good agreement between our predictions and experiment for bent waveguides in this geometry. [S0163-1829(97)04416-0]

I. INTRODUCTION

It is possible to produce very narrow two-dimensional conducting surfaces, or "quantum wires," which allow electrons to propagate in the channels formed by these surfaces, but require the electron wave function to vanish on the boundary of the surface. As the width of these quantum wires is roughly equal to the de Broglie wavelength of a cold electron, wave effects will dominate the physics of these systems. Quantum wires have been used extensively to study quantum interference effects.¹⁻⁵ The simplest model is a surface of infinite extent with a bend in the center and open straight ends. Such surfaces have no "classically forbidden" region (a classical particle could roll freely through such a system), so the discovery by Schult, Ravenhall, and Wyld⁶ (and earlier by Lenz *et al.*⁷) that such systems possess a bound state was rather surprising. Goldstone and Jaffe⁸ (and Exner^{9,10}) then proved the remarkable result that at least one bound state exists for *all* two-dimensional surfaces of constant width (except surfaces of constant curvature, which have no bound state). As is well known, a "bulge" in a two-dimensional surface can be mapped into one dimension; the transverse bulge then appears as an effective local attraction, which in one dimension always produces a bound state.

However, it was surprising to find that a bend produces an effective attraction similar to a bulge.

The existence of these bound states can be understood qualitatively. Consider a quantum wire containing a bend. In previous papers^{11,12} we examined the properties of systems containing a single bend. In this paper we will examine the case of a system with two right-angle bends as shown in Fig. 1. The width of the straight sections is W and the height of the bend is H . For the moment consider the case where the straight sections of the wire are infinitely long. The wave function for the electron satisfies the equation

$$(\nabla^2 + k^2)\psi(x, y) = 0, \quad \psi|_S = 0. \quad (1.1)$$

In Eq. (1.1), the wave number k is related to the energy E by $k^2 = 2m^*E/\hbar^2$. In either straight section the requirement that the wave function vanish on the boundary, and the separability of the Hamiltonian, forces the y dependence of the wave function to be of the form $\sin(n\pi y/W)$ for integer n . This transverse quantization condition produces an energy threshold; the lowest energy allowed for free propagation is $E_{\text{thr}} = (\hbar\pi)^2/(2m^*W^2)$. Both the extra space in the bend(s) of the wire, and the bending itself, produce an effective attraction which supports electron bound state(s) in the region of the bend(s). The wire of Fig. 1 will have one or two bound

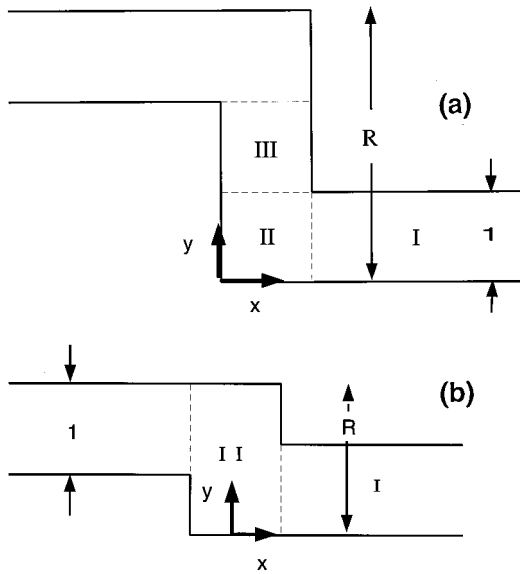


FIG. 1. Simplified model for bent quantum wire. Infinitely long wire with two right-angle bends, the width arbitrarily normalized to 1 and the aspect ratio (height/width ratio) R . (a) The aspect ratio $R > 2$ is the “quantum bend discontinuity” case of Ref. 17. For the purpose of calculations the wire is divided into three sections labeled *I*, *II*, and *III*, respectively. (b) The aspect ratio $1 < R < 2$ is the “quantum bend continuity” case. The wire is divided into sections labeled *I* and *II*, respectively.

states, which appear as isolated states with energy below E_{thr} . The bound state wave functions will be largest in the vicinity of the bend, and fall off exponentially with the distance from the bend region.

Bent quantum wires are thus examples of quantum systems whose bound states do not arise from the “traditional” picture, where a binding potential creates classically allowed and forbidden regions. Here the boundary conditions (vanishing of the wave function on the boundaries of the wire) give rise to transverse quantization conditions which produce a minimum threshold energy for continuum solutions. Localized bends or bulges in these wires then produce effective local attractive forces which give rise to bound states. As the effective attraction in a bent wire is (to lowest order) proportional to the square of the curvature of the wire,⁸ the magnitude of the binding energy increases as the curvature increases.

In previous papers^{11,12} we have considered bent two-dimensional systems and their analogy to rectangular waveguides. If one constructs some two-dimensional curve σ in the xy plane, which possesses a scalar field ψ satisfying the Helmholtz (or Schrödinger) equation $[\nabla^2 + k^2]\psi = 0$, with $\psi|_S = 0$ on the boundary S of the curve, then one can produce a rectangular waveguide by translating the curve σ normally in the z direction. E and B fields can be constructed from ψ as follows:

$$\mathbf{E}(x, y) = ik\hat{\mathbf{z}}\psi(x, y), \quad \mathbf{B}(x, y) = -\hat{\mathbf{z}} \times \nabla\psi. \quad (1.2)$$

The E and B fields of Eq. (1.2) will satisfy Maxwell’s equations and boundary conditions for TE modes in the waveguide,¹³ where the electron wave number k is related to the frequency $f = \omega/2\pi$ by

$$k \rightarrow \frac{2\pi\sqrt{\mu\epsilon}f}{c}. \quad (1.3)$$

Therefore if there exist bound states of the Schrödinger equation for particles moving in the two-dimensional curve σ (i.e., solutions of the wave equation below the minimum energy for free propagation of waves in the wire), there will be analogous confined TE modes (solutions of E and B fields with frequencies below the cutoff frequency for the waveguide), and the confined \mathbf{E} field of Eq. (1.2) will be described by the same scalar function ψ which constitutes the bound state wave function of the electron in the quantum wire, in Eq. (1.1).

In our previous work, rectangular waveguides were constructed and both bound states and E - M fields were measured.^{11,12} Microwaves were pumped into the center of bent waveguides, and the ratio of reflected to incident power was measured there. At the frequency corresponding to the confined state, a sharp minimum was observed in the reflected power, representing resonant absorption of microwave power. At other frequencies below cutoff almost 100% of the power was reflected back to the generator. The fields were measured by moving a small metal sphere inside the waveguides, and observing the shift in resonant frequency as a function of the position of the sphere in the waveguide. Both bound state positions and fields were found to agree very well with theoretical predictions.

Although one can demonstrate experimentally the presence of electron bound states in bent quantum wires, it is not easy to measure the details of electron wave functions in such small systems. In this paper, we investigate an alternative method for studying the detailed properties of bound states in bent systems. Theoretically, we derive the transmission coefficients for free particles in bent two-dimensional systems. Experimentally, we measure the properties of confined \mathbf{E} fields in bent rectangular waveguides. We construct rectangular waveguides with two bends, and we locate and measure confined TE modes in such waveguides. Having found the confined modes, we map out the resulting electromagnetic energy density in the waveguide.

Because of the one-to-one correspondence between eigenfunctions for waves in two-dimensional surfaces and TE modes in waveguides of the same shape, the observation of confined TE modes in waveguides below the cutoff frequency predicts the existence of bound electron states in bent quantum wires. Furthermore, the electric field we measure is identical to the wave function for the electron bound states in a quantum wire of the same geometry as the waveguide. We show that the mapped fields, and location of confined modes in the waveguides, agree quite well with our theoretical predictions.

We focus our attention on the case of a quantum wire with two right-angle bends, as shown schematically in Fig. 1. In this paper, we show how the number of bound states, binding energies, and properties of the eigenfunctions depend on the geometry of systems with two bends.

Quantum wires with this geometry have been the subject of both experimental and theoretical investigations. Wu *et al.*¹⁴ constructed quantum wires with double right-angle bends, with a shape essentially that of Fig. 1. They measured conductance vs gate voltage in such structures, and observed

at least one peak in conductance below the threshold for free electron conduction. They interpreted these peaks as electrons tunneling through impurity sites in the constriction, as was discussed by McEuen *et al.*,¹⁵ who measured conductance vs gate voltage for electrons in a straight quantum wire.

This conclusion was challenged by Wang and collaborators.^{16,17} They carried out theoretical calculations of conductance in quantum wires with two bends,¹⁶ and with $2N$ bends.¹⁷ These authors claim that the subthreshold peak(s) observed by Wu and collaborators are due to electrons tunneling through bound states in the wire.

In this paper, we concentrate on the location and properties of the bound states in a waveguide or quantum wire with two right-angle bends. Our paper is organized as follows. In Sec. II we calculate bound state energies and transmission coefficients for this geometry. At this stage we make the simplifying assumption that the legs of the wire are infinitely long. In this case, we show that all properties of the bound states are determined by the aspect ratio R of the wire (the ratio of the height of the wire to its width, shown schematically in Fig. 1). In Sec. III we discuss the experimental measurement of states in a rectangular waveguide with two bends, and we compare the experimental results with our theoretical predictions. In Sec. IV we draw conclusions and discuss possible future experiments.

In the following paper,¹⁸ we apply the theoretical techniques outlined in this paper to the calculation of conductance for electrons in bent quantum wires. The situation is more complicated than the simple model used in this paper. We must take into account the finite length of the wires, consider the effect of the applied gate voltage on the conductance, and consider the many physical effects which occur in scattering above the conductance threshold. The signature of bound states in such systems is transmission below the minimum energy for free propagation, due to electron tunneling through the bound states. In this second paper, we compare our results with both the data of Wu *et al.* and the theoretical calculations of Wang and collaborators.

II. BOUND STATES FOR ELECTRONS IN BENT TWO-DIMENSIONAL SYSTEMS

We consider the case of a quantum wire with two right-angle bends. A useful first approximation is to examine the case of an infinitely long two-dimensional system with two bends, as shown in Fig. 1. We define the horizontal and vertical directions as x' and y' , respectively, and the width and height of the wire are W and H . The electron wave function in the quantum wire satisfies the Schrödinger equation $-\hbar^2/2m^*[(\partial^2/\partial x'^2) + (\partial^2/\partial y'^2)]\psi(x', y') = E\psi(x', y')$, where m^* is the electron effective mass. With no loss of generality, we can transform to the dimensionless coordinates,

$$x = x'/W; \quad y = y'/W; \quad R = H/W,$$

$$k^2 = \frac{2m^*EW^2}{\hbar^2}. \quad (2.1)$$

In the coordinates (x, y) , the electron wave function $\psi(x, y)$ satisfies the Helmholtz equation $(\nabla^2 + k^2)\psi(x, y)$

$= 0$. Here the dimensionless quantity $R = H/W$, the length of the straight section between the two bends, is the aspect ratio of the wire.

From the theorems of Exner^{9,10} and Goldstone and Jaffe,⁸ such a system is guaranteed to have at least one bound state. The wave functions for an electron in a quantum wire can be obtained by many different techniques; series expansions,^{11,19,20} relaxation methods,¹² transfer matrix methods,²¹ or the quantum transmitting boundary method.²² We use a series expansion method to calculate the bound state wave functions. Note that the right half of the wire can be mapped onto the left-half side by reflection about the lines $x = 1/2$ and $y = R/2$. Since the Hamiltonian is symmetric under these reflections, the eigenfunctions for this system are either symmetric or antisymmetric under this transformation. Therefore we need solve for the wave function on half the wire, and impose the correct symmetry on the eigenstates.

For infinitely long wires, the properties of the bound states are a function only of the aspect ratio, R . Wang and collaborators^{16,17} divide these bent wires into two categories. When $R < 2$, as shown in Fig. 1(b), it is possible for an electron to travel in a straight line path through the wire. They call this a ‘‘double bend continuity.’’ For $R \geq 2$, no straight line path is possible. They call this geometry a ‘‘double bend discontinuity.’’

We will first examine the case when the aspect ratio $R \geq 2$, the ‘‘double bend discontinuity’’ case of Wang and collaborators; this is shown schematically in Fig. 1(a). We will outline the solution here; the solution in the case $1 < R < 2$ is given in the Appendix. We solve for the bound states in the wire by dividing it into three sections as shown in Fig. 1(a). Region *I* is defined by $[x \geq 1, 0 \leq y \leq 1]$; we expand the wave function ψ_I in Cartesian coordinates, where the wave function boundary conditions are

$$\psi_I(x, y)|_{y=0} = \psi_I(x, y)|_{y=1} = 0; \quad \psi_I(x, y) \xrightarrow{x \rightarrow \infty} 0. \quad (2.2)$$

Separation of variables in Cartesian coordinates then gives the series solution

$$\psi_I(x, y) = \sum_{n=1}^{\infty} A_n \sin(n\pi y) e^{-\alpha_n x}, \quad (2.3)$$

where $\alpha_n = \sqrt{n^2\pi^2 - k^2}$.

Region *II* is defined by $[0 \leq x \leq 1, 0 \leq y \leq 1]$. In region *II* the boundary conditions are

$$\psi_{II}(x, y)|_{y=0} = \psi_{II}(x, y)|_{x=0} = \psi_{II}(x, y)|_{x=y=1} = 0. \quad (2.4)$$

The following wave function satisfies the boundary conditions of Eq. (2.4) in this region:

$$\psi_{II}(x, y) = \sum_{n=1}^{\infty} [B_n \sin(n\pi y) \sinh(\alpha_n x) + C_n \sin(n\pi x) \sinh(\alpha_n y)]. \quad (2.5)$$

Region *III* is defined by $[0 \leq x \leq 1, 1 \leq y \leq R - 1]$. In region *III* the boundary conditions for the symmetric (*S*) and anti-symmetric (*A*) wave functions are

$$\begin{aligned}\psi_{III}(x,y)|_{x=0} &= \psi_{III}(x,y)|_{x=1} = 0, \\ \psi_{III}^S(1-x,R-y) &= \psi_{III}^S(x,y), \\ \psi_{III}^A(1-x,R-y) &= -\psi_{III}^A(x,y).\end{aligned}\quad (2.6)$$

The following wave function satisfies the boundary conditions of Eq. (2.6) in this region,

$$\psi_{III}(x,y) = \sum_{n=1}^{\infty} D_n \sin(n\pi x) F_n[\alpha_n(y-R/2)], \quad (2.7)$$

where

$$\begin{aligned}\mathbf{T}_{nk} &= \frac{k\pi(-1)^k d_{nk}}{\alpha_n \{ \sinh(\alpha_n) F_{n+1}(\alpha_n[1-R/2]) / F_n(\alpha_n[1-R/2]) - \cosh(\alpha_n) \}}, \\ \mathbf{S}_{nk} &= \frac{(-1)^{k+1} k\pi \exp(-\alpha_n) d_{nk}}{\alpha_n}, \\ d_{nk} &= \frac{(-1)^{n+1} 2n\pi \sinh(\alpha_k)}{\alpha_k^2 + (n\pi)^2}.\end{aligned}\quad (2.9)$$

The bound states occur at those values of k^2 for which $\text{Det}|\mathbf{Z}(k^2)|=0$. Once we have found the relevant values of k^2 , we can determine the expansion coefficients and reconstruct the wave functions ψ for each bound state. In our calculations we have truncated our expansion at $N=10$. We find that both the bound state energies and wave functions are stable and relatively accurate with this small number of expansion coefficients.

In Fig. 2 we show the bound state energies as a function of the aspect ratio R . The continuum begins at $k^2 = \pi^2$ [see Eq. (2.3)]; therefore we plot the parameter $\epsilon = k^2/\pi^2$. As $R \rightarrow 1$, $\epsilon \rightarrow 1$. For $R < 2.5$, only the symmetric state is bound; the antisymmetric state is unbound for smaller values of R . The bound state wave function has a single peak centered in the middle of the double bend; in Fig. 3(a) we plot the density contours for the symmetric bound state corresponding to $R=2$. As R increases from 1, the binding energy increases, reaching a maximum for $R \approx 1.7$. As R increases further, the binding energy then decreases. For $R > 2.5$, both symmetric and antisymmetric bound states appear. Both the symmetric and antisymmetric bound state wave functions have a peak at each bend of the quantum wire. In Figs. 3(b) and 3(c), we plot the wave function contours for the symmetric and antisymmetric bound states, respectively, when $R=3$.

For very large values of R we see from Fig. 2 that both symmetric and antisymmetric bound states approach the same energy, $\epsilon \approx 0.930$ (this value of ϵ corresponds to the bound state energy for an infinitely long wire of unit width with a single right-angle bend¹¹). In this case, the bound state wave function is very small except for one peak in each right-angle bend; in Figs. 4(a) and 4(b) we show density plots for the symmetric and antisymmetric bound states, respectively, when $R=6$.

$$\begin{aligned}F_n^S(t) &= \cosh(t) \quad (n \text{ odd}) = \sinh(t) \quad (n \text{ even}), \\ F_n^A(t) &= \sinh(t) \quad (n \text{ odd}) = \cosh(t) \quad (n \text{ even}).\end{aligned}\quad (2.8)$$

The coefficients are determined from the conditions that ψ and its normal derivatives be continuous at the boundaries between regions *I*, *II*, and *III*.

To solve, we truncate the (infinite dimensional) expansions at N basis functions. The resulting equations can be expressed as an $N \times N$ matrix equation; it is straightforward to show that the condition for a bound state is $\text{Det}(\mathbf{Z})=0$, where $\mathbf{Z} \equiv \mathbf{TS} - \mathbf{1}$, and

The number of bound states, and their locations, are completely determined by the geometry of the bent quantum wire. We are studying the case of a long wire with two right-angle bends. Provided that the length of the quantum wire with two bends is much longer than the other dimensions, the bound state properties are completely determined by the width W of the wire and the aspect ratio $R=H/W$. For $R < 2.5$, there is only a single bound state; for $R > 7$, the two bound state energies coalesce so that the symmetric and antisymmetric states appear at essentially the same energy.

Wang, Berggren, and Ji¹⁶ and Wang¹⁷ studied electron

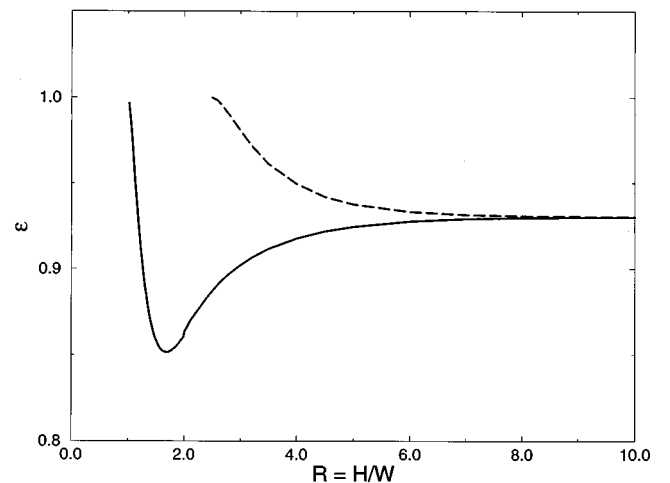


FIG. 2. Bound state eigenvalues in bent quantum wire of Fig. 1, as a function of the aspect ratio $R=H/W$. The bound state energy is defined as $E \equiv (\hbar\pi)^2 \epsilon / (2m^*W^2)$. Plot of ϵ vs R for bound states in wire. Solid curve: symmetric bound states; dashed curve: antisymmetric bound states.

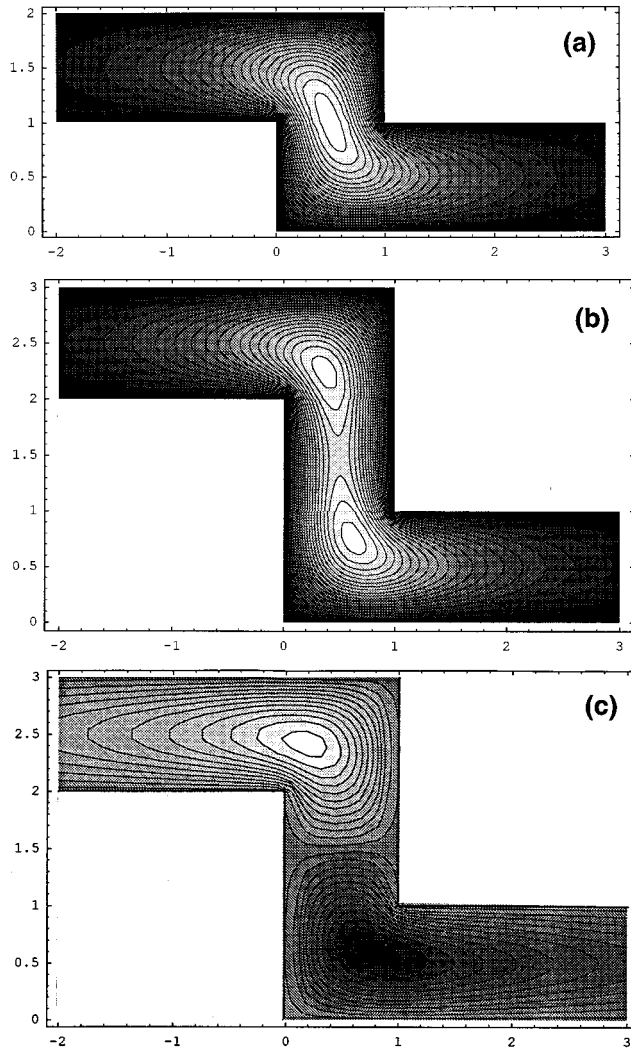


FIG. 3. Calculated contour plots for amplitudes of bound state wave functions in a long wire with two bends. (a) Symmetric bound state with the aspect ratio $R=2$; (b) symmetric bound state for wire with the aspect ratio $R=3$; (c) antisymmetric bound state for wire with $R=3$. The positive values of the wave function have the lightest shading; shading becomes progressively darker as the value of the wave function decreases.

conductance in quantum wires with two bends. They examined electron tunneling through bound states in these quantum wires. Many of our results agree with the conclusions of Wang and collaborators. We agree that for sufficiently large values of aspect ratio R , both the symmetric and the antisymmetric bound state wave functions are peaked in the corners of the wire. We also find that with increasing R , the distance in energy between the symmetric and antisymmetric states decreases.

However, we disagree with Wang and collaborators in one respect. They state that all “double bend discontinuity” geometries, i.e., all wires with aspect ratio $R>2$, should have both a symmetric and an antisymmetric bound state. As can be seen from Fig. 2, no true antisymmetric bound state exists for $R<2.5$; for these geometries, the antisymmetric state is in the continuum.

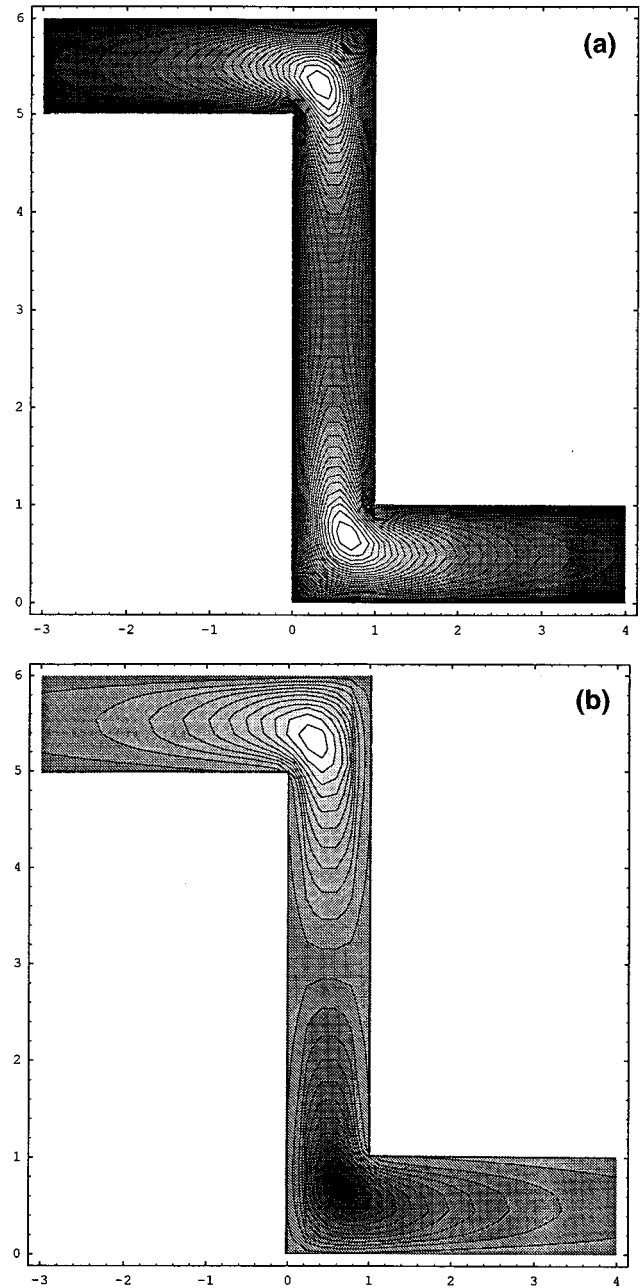


FIG. 4. Contour plots for amplitudes of bound state wave functions in long wire with two bends. (a) Symmetric bound state with the aspect ratio $R=6$; (b) antisymmetric bound state for wire with $R=6$. The notation is that of Fig. 3.

III. EXPERIMENTAL MEASUREMENTS OF CONFINED MODES IN BENT WAVEGUIDES

A. Experimental techniques

As we discussed in the Introduction, we can construct a rectangular waveguide with two bends, whose cross sectional area is given by Fig. 1. Maxwell’s equations for TE modes in this waveguide are satisfied by E and B fields which have the form $\mathbf{E}=ik\hat{\mathbf{z}}\psi(x,y)$, $\mathbf{B}=-\hat{\mathbf{z}}\times\nabla\psi(x,y)$.¹³ The scalar field $\psi(x,y)$ satisfies the Helmholtz equation $[\nabla^2+k^2]\psi(x,y)=0$, with $|\psi|_S=0$ on the boundary S of the

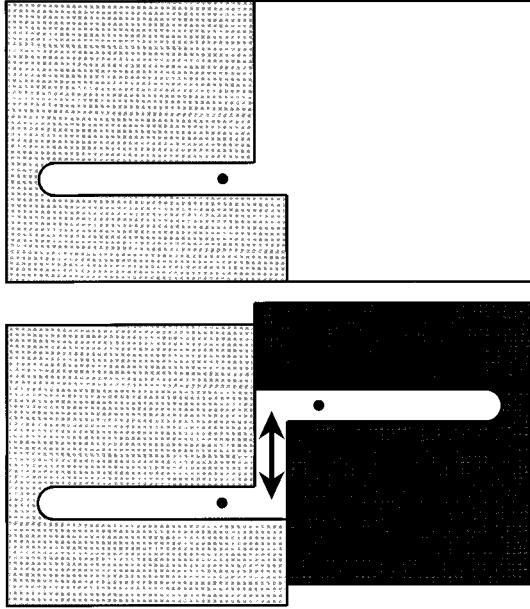


FIG. 5. Schematic view of the waveguide structure used in the experiments. The structure was made from two half-inch aluminum plates. Top: one of the machined aluminum plates; the other is its mirror image. The shaded area is 0.635 cm higher than the lighter area. The black dot is a clearance hole for a coaxial cable. Bottom: schematic view of the assembled structure. The space between the two plates, shown in white, forms the double bend structure. The waveguide width is $W=1.905$ cm. The distance between the bends is continuously variable by sliding the two plates along the axis indicated by the double arrow.

waveguide. The relation between the wave number k and frequency is given in Eq. (1.3).

The scalar field ψ for the waveguide is exactly the solution of the Schrödinger equation for an electron in a quantum wire, as given in Eq. (1.2). Therefore, since there exist bound states of the Schrödinger equation in the bent quantum wire, there will be analogous confined TE modes below the cutoff frequency for the waveguide, and the confined E field will be completely described by the quantum wire bound state wave function ψ .

To observe the confined electric fields in an electromagnetic waveguide with two right-angle bends, we constructed a finite version of the waveguide structure schematically shown in Fig. 1. With this system, we could continuously vary the aspect ratio, $R=H/W$ over the range $1 < R < 6$, measure the frequencies for the bound states, and map the electromagnetic energy density for the bound states.

The structure was made of two pieces of machined aluminum. Figure 5 (top) shows one of the pieces; the other is its mirror image. The darkly shaded area is 0.635 cm higher than the lighter areas. When the second piece is inverted, the empty space between the plates forms a waveguide double bend, as shown in the bottom part of the figure. The waveguide width is $W=1.905$ cm, and its depth is $D=0.635$ cm. Relative motion of the two plates in the direction of the double arrow produces a continuous variation of H while keeping W fixed. The joints at the outside corners of the waveguide bends do not affect the modes because both the

electric and magnetic fields vanish at such a corner. However, since microwave surface currents flow elsewhere between the two plates, the waveguide structure must be clamped together to ensure good electrical contact.

In such a structure, propagating waves with frequencies below $c/2D$ ($=23.6$ GHz here) must only have a nonzero component of the electric field perpendicular to the large plates in order to satisfy the boundary conditions on the surrounding conducting surfaces. The magnetic field must be in the xy plane.

We measured the resonant frequencies using the same method as we have previously described.¹² Small holes (the black dots in Fig. 5, just outside the bends) provide clearance for 0.141" semirigid coaxial lines. We place a coaxial line (with its center conductor extending about 0.5 cm to form an antenna) through one of the holes. We can vary the degree to which the line radiates into the waveguide structure by the amount of protrusion of the antenna. A Hewlett-Packard 8510B network analyzer connected to the coax sends the microwave power to the antenna and measures the reflected power as a function of frequency. Sharp drops in the reflected power occur for the bound state frequencies.¹¹

The cutoff frequency for the lowest propagating mode in the waveguides, TE_{01} , is nominally $c/2W=7.87$ GHz. We determine the actual cutoff frequency experimentally by adjusting our structure so that $R=1$ to form a long, straight cavity with the same width, W , and a length, $L=27.30$ cm. We then measure the frequencies of the first few TE_{01p} modes, $f(p)$. A linear fit to the data $[f(p)]^2=f_{co}^2+p^2(c/2L_{eff})^2$, gives $f_{co}=(7.850\pm 0.003)$ GHz and $L_{eff}=27.05$ cm (the ends of the cavity are rounded with radii $=0.953$ cm, which makes L_{eff} somewhat shorter than the physical length).

Once we can measure the resonant frequency, we can map out the field distribution for the bound states for a few representative values of R . The simple two-dimensional mapping procedure is a technique which has been known for some time,²³ and which has been beautifully refined by Sridhar.²⁴ In this method the resonance is perturbed with a small steel ball (1/8" diameter) located at a known position within the waveguide bend and then the change in the resonant frequency of the mode as a function of position, $\Delta f(x,y)$ is measured. We locate the steel ball (with a precision of about 1 mm) on the vertices of a 0.3175 cm two-dimensional grid with a small magnet.

In a previous paper¹² we derived a formula for the perturbation in the resonant frequency produced by the presence of a metal ball of radius r :

$$\frac{\Delta f(x,y)}{f_0} = -\frac{4\pi r^3}{2DW^2} \left(C|\psi(x,y)|^2 - \frac{1}{2k^2} \left[\left| \frac{\partial \psi(x,y)}{\partial x} \right|_2 + \left| \frac{\partial \psi(x,y)}{\partial y} \right|_2 \right] \right). \quad (3.1)$$

In Eq. (3.1), ψ is the normalized wave function associated with the bound state being measured. The dimensionless constant, C , depends on the relative size of the ball and the depth of the waveguide, D , but is greater than 2.4 in general.

Moving the steel ball allows us to map out the electric and magnetic fields in the structure, as the positions of the ball

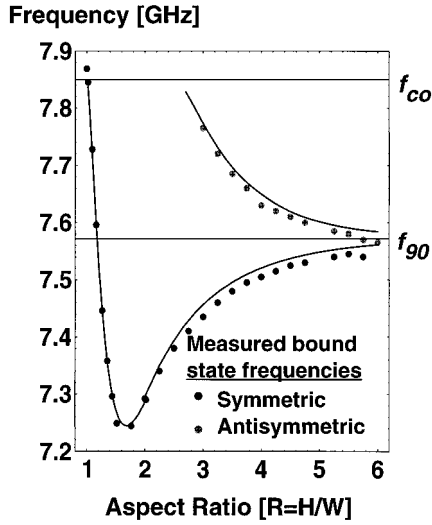


FIG. 6. Bound state frequencies as a function of the aspect ratio $R=H/W$ in the double bend waveguide structure of Fig. 5. The symbols represent the experimental results for the symmetric (filled circles) and antisymmetric states (open circles). The lines represent the theoretically determined resonant frequencies calculated from the ratio of the bound state energy and the threshold energy for free propagation: $f_{\text{bound}}=f_{\text{co}}(E_{\text{bound}}/E_{\text{thr}})^{1/2}$. The TE_{01} cutoff frequency, f_{co} , was determined to be 7.85 GHz and is shown by the solid horizontal line. The theoretical value for the bound state frequency of an isolated 90° bend of the same width ($f_{90}\approx 0.966f_{\text{co}}$) is indicated by the dashed horizontal line.

that produce local minima in the resonant frequency of a mode correspond to antinodes of the electric field for that mode, and positions that produce local maxima in the resonant frequency correspond to antinodes of the transverse magnetic field strength.

B. Bound state frequencies as a function of R

In Fig. 6 we plot the experimental values for the symmetric and antisymmetric bound state eigenvalues as a function of the aspect ratio R of the bent waveguide. We observe a symmetric bound state below the cutoff frequency (f_{co} , indicated by the solid horizontal line) for all values of $R>1$. We observe an antisymmetric bound state for $R\geq 3$. As we had predicted (see Fig. 2), for large values of R the symmetric and antisymmetric frequencies approach each other closely. For $R<2$, the symmetric bound state frequency has a minimum and then rapidly increases to the cutoff frequency as $R\rightarrow 1$. For $R<4$, the antisymmetric frequency rapidly approaches f_{co} and we cannot follow the state below $R=3$. However, it certainly follows our theoretical results, which predict that no antisymmetric bound state will exist for $R<2.5$.

The theoretical values are plotted as dashed lines in the figure. These are calculated as $f_{\text{bound}}=f_{\text{co}}(E_{\text{bound}}(R)/E_{\text{thr}})$, where $E_{\text{bound}}(R)$ are the calculated bound state energies, and $E_{\text{thr}}=(\hbar\pi)^2/(2m^*W^2)$ (these are the curves shown in Fig. 2). For large values of R , both frequencies approach the bound state frequency for an isolated 90° bend (about $0.966f_{\text{co}}$).¹¹ The shapes of the theoretical curves and a line

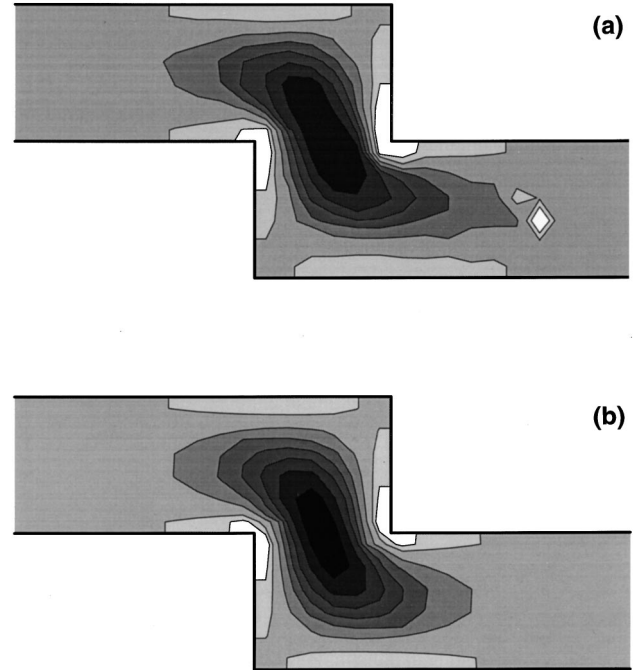


FIG. 7. (a) Experimentally measured contour plot of the resonant frequency shift for the double bend waveguide structure with the aspect ratio $R=2.0$. The shading is light for the positive frequency shift (relatively large magnetic field energy density) and dark for the negative frequency shift (relatively large electric field energy density). There is a single maximum in the electric field energy density centered between the two bends. (b) Theoretical prediction for the contour plot of the resonant frequency shift for the bound state for $R=2$ as predicted from Eq. (3.1).

drawn through the data points are nearly identical. A shift in the value of the cutoff frequency of 0.013 GHz puts the theoretical line on top of the data points. We do not understand the source of this shift, but it amounts to less than $1/500$ of f_{co} .

C. Mapping the bound states

In Fig. 7(a), we show the results of field mapping in a waveguide with two bends where the aspect ratio is $R=2$. In this case, there is only a single confined mode. The E field for this mode is symmetric about the center of the waveguide, with a single peak in the center and an exponential decrease along the legs of the waveguide [this corresponds to the case shown in Fig. 3(a)]. The underlying grid of data had a spacing of $1/6$ of the waveguide width. The graph is shaded so that darker (lighter) regions are those with a negative (positive) frequency shift (e.g., regions of relatively large electric field energy density appear darkest and those of large magnetic field energy density appear lightest). The largest electric energy density occurs centered between the two bends. The largest magnetic energy density occurs where the surface current densities are greatest near the adjacent side walls of the waveguide, and also near the location of the antenna, on the right waveguide section.

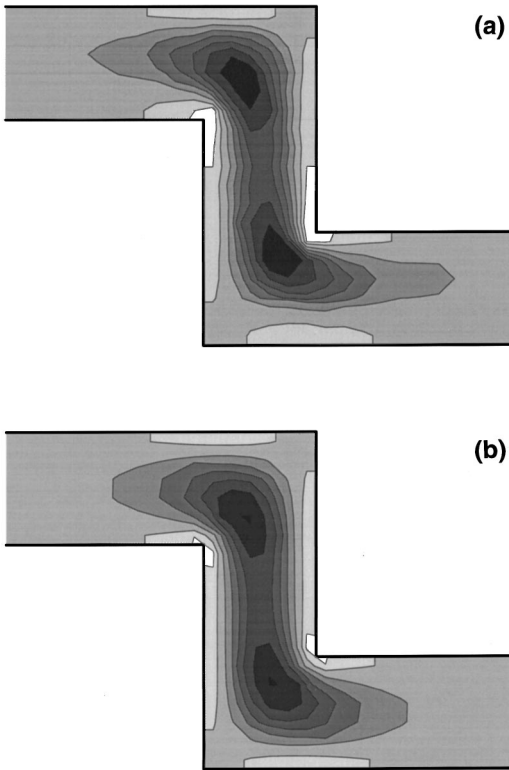


FIG. 8. (a) Experimentally measured contour plot of the resonant frequency shift for the lower frequency confined state in a double bend waveguide structure with the aspect ratio $R=3.0$. This state is symmetric about the center of the waveguide. (b) Theoretical prediction for the contour plot of the resonant frequency shift for the symmetric bound state for $R=3$. The notation is that of Fig. 7.

In Fig. 7(b) we show the theoretical calculations for the resonant frequency shift using Eq. (3.1) with $r^3/(DW^2)=1/576$ and $C=2.46$.¹² Comparing the two halves of the figure, we find excellent quantitative and qualitative agreement between theory and experiment. The only place where there appears to be a systematic difference between theory and experiment is down the straight legs of the waveguide, where the experimental measurements fall off somewhat less rapidly than theory. The theory predicts a maximum electric energy density approximately 10% greater than found in our experiment, so that the theoretical plot has one more dark contour than the experimental result.

In Fig. 8(a) we show the field mapping for the symmetric bound state wave function corresponding to aspect ratio $R=3$. For this case we predict a peak of the electric field at each of the corners of the wire [this corresponds to the situation shown in Fig. 3(b)]. These peaks are seen clearly in the data. Again, there is excellent quantitative agreement between the theory, as shown in Fig. 8(b), and experiment.

In Fig. 9(a) we show experimental results for the field mapping for the antisymmetric bound states in a wire with $R=3$ [this is the case shown in Fig. 3(c)]. The bound state wave function for this configuration has a single node near the center of the waveguide. Once again, the experimental measurements are very close to the theoretical predictions shown in Fig. 9(b). Comparing the shapes of the symmetric (Fig. 8) and the antisymmetric states with $R=3$, we see that

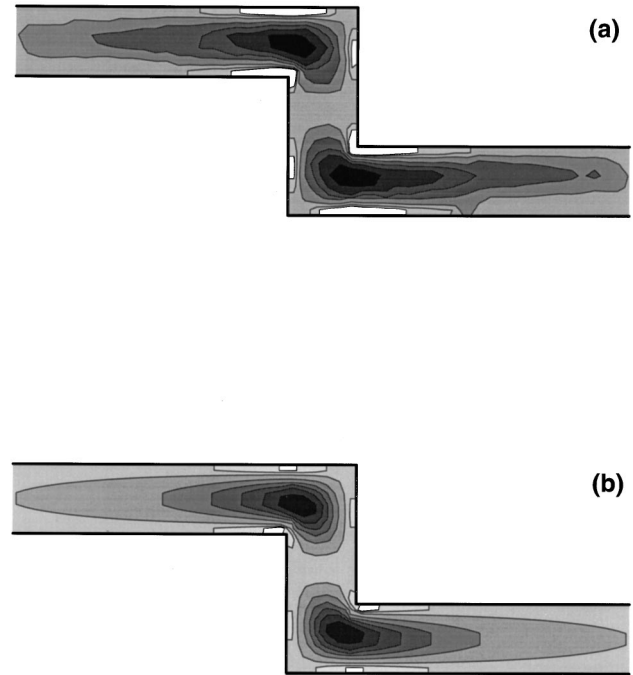


FIG. 9. (a) Experimentally measured contour plot of the resonant frequency shift for the antisymmetric confined state in the double bend waveguide structure with the aspect ratio $R=3.0$. Note the node in the electric energy density centered between the two bends. (b) Theoretical prediction for the contour plot of the resonant frequency shift for the antisymmetric bound state for $R=3$. The notation is that of Fig. 7.

the antisymmetric state extends much farther down the straight sections. The antisymmetric frequency is much closer than the symmetric frequency to the cutoff frequency for the TE_{01} propagating mode, and therefore has a much longer decay length in the waveguide.

IV. CONCLUSIONS

In the past few years it has been realized that quantum particles moving in bent two-dimensional systems should generally exhibit bound states, which arise from the bends in the system. Thus, electrons moving in narrow “quantum wire” structures should possess bound states. Recently, it has been possible to demonstrate experimentally the existence of these states. However, the size of these systems makes it difficult to obtain detailed measurements of the properties of electrons in such bound states. In this paper, we make model calculations of such bent structures, and we compare our predictions with experimental data for a certain geometry.

We first derived formulas for wave functions in quantum wires with two right-angle bends. From these formulas one can determine the number and location of bound states. The bound states have the following properties, which can be seen from Fig. 2: for $1 < R < 2.5$, only the symmetric bound state exists. For $1 < R < 1.7$, the binding energy increases as the aspect ratio increases; for larger values of R , the binding energy of the symmetric (antisymmetric) state decreases (increases) with increasing R . For large values of R , the antisymmetric and symmetric binding energies asymptotically

approach the identical value $\epsilon \approx 0.930$; this is the binding energy for a wire with a single right-angle bend.

Because of the limited data for these quantum wires, we used the one-to-one correspondence between wave functions for electrons moving freely in a quantum wire, and the electric field for TE modes in a rectangular waveguide, whose cross-sectional area has the same shape as the quantum wire. Electron bound states are characterized by wave functions which are localized in the vicinity of the bend, and which fall off exponentially with distance along the wire. The corresponding electric fields produce electromagnetic field modes below the cutoff frequency for the waveguide; the electric fields are also localized around the bend region and should fall off exponentially away from the bend region.

Having shown this correspondence, we constructed waveguides with this shape, and we demonstrated the location of the confined states by measuring the ratio of reflected to incident power $R(f)$ as a function of frequency f for microwaves. The bound state appeared at that frequency where a sharp minimum in $R(f)$ was observed. The field distributions inside these waveguides were measured by moving a small metal sphere inside the waveguide and observing the shift in resonant frequency as a function of the position of the sphere. Although this process measures a combination of the E_z and H_t fields, the maximum and minimum frequency shifts correspond to antinodes of H_t and E_z , respectively.

We also derived a simple formula which related the resonant frequency shift to the electric and magnetic field densities in the waveguide. Qualitatively we obtained good agreement between theory and measurements. Quantitatively, we found very good agreement between theoretical predictions of the maximum frequency shifts (antinodes in H_t); however, theoretical predictions of the minimum frequency shifts overpredicted experimental results by 25–35 %.

Perhaps the most interesting thing about such states in bent waveguides is that they do not seem to have been predicted or measured until the past few years,^{11,12} despite decades of research on the properties of waveguides. In most waveguides the practical interest is in the transmission and reflection well above the cutoff frequency, and the presence of confined states below the cutoff frequency will have an influence on transmission properties of states above the cutoff.

Experimental studies have been carried out for quantum wires with two bends by Wu and collaborators.¹⁴ Wang and collaborators^{16,17} carried out theoretical calculations of the conductance for electrons in this geometry, and compared it to these experimental results. The geometry of our waveguides was chosen to correspond to that studied by Wu *et al.* and Wang. In the following paper,¹⁸ we will extend our discussion to treat the conductance in quantum wires of this geometry. By comparing our results to those of Wu *et al.* and Wang, and using our understanding of such systems obtained from our work with waveguides, we will assess the role played by the electron bound states of those quantum wires on the observed conductance near threshold.

In conclusion, we have shown that theoretical calculations give very good agreement with experiments of confined electromagnetic fields in bent waveguides. We showed that the number of confined electric field modes (i.e., bound states), and their locations, are determined by the geometry of the



FIG. 10. Contour plot of the calculated wave function for the electron bound state in wire with the aspect ratio $R=1.5$, showing a single maximum in the center of the bend region.

waveguide. We also showed that the electric and magnetic fields in such confined modes could be accurately predicted from theory. This gives us confidence in applying the same theoretical techniques to electron conductance in quantum wires of the same geometry.

ACKNOWLEDGMENTS

The work in this paper was supported in part by the NSF under Contract Nos. NSF-PHY-9408843 and NSF-DMR-9423088. One of the authors (J.P.C.) acknowledges support from the Alfred P. Sloan Foundation. One author (J.T.L.) thanks R.L. Jaffe for interesting conversations about the properties of these systems, and about results that he and J. Goldstone had derived. One of the authors (D.P.M.) thanks the Indiana University Nuclear Theory Center for its hospitality while this paper was being written. Two of the authors (D.T. and C.N.Y.) thank the Indiana University Cyclotron for its hospitality under the Research Experiences for Undergraduates (REU) program, sponsored by NSF Contract No. NSF-PHY-9423896.

APPENDIX: BOUND STATES IN A BENT WIRE WHEN $1 < R < 2$

To find bound states and wave functions in a bent quantum wire when the aspect ratio R is in the range $1 < R < 2$, the boundary matching conditions outlined in Sec. II must be modified. In Fig. 1(b) we show a picture of such a wire, which we have divided into three regions. The wave function must be either symmetric or antisymmetric under reflection about the lines $x=0$ and $y=R/2$. The bound state wave functions will be symmetric under these reflections, consequently we need only solve for the wave functions in regions I and II. Wave functions satisfying the appropriate boundary and symmetry conditions have the form

$$\begin{aligned} \psi_I(x,y) &= \sum_{n=1}^{\infty} A_n \sin(n\pi y) e^{-\alpha_n x} \quad (x \geq 1/2, \quad 0 \leq y \leq R), \\ \psi_{II}(x,y) &= \sum_{n=1}^{\infty} B_n \sin\left(\frac{n\pi y}{R}\right) \cosh(\beta_n x) \quad (n \text{ odd}) \\ &= \sum_{n=1}^{\infty} B_n \sin\left(\frac{n\pi y}{R}\right) \sinh(\beta_n x) \quad (n \text{ even}) \\ & \quad (-1/2 \leq x \leq 1/2, \quad 0 \leq y \leq R). \end{aligned} \quad (\text{A1})$$

In Eq. (A1), we have $\alpha_n = \pi \sqrt{n^2 - \epsilon}$ and $\beta_n = \pi \sqrt{n^2/R^2 - \epsilon}$.

The condition for bound states is obtained by matching the wave functions and normal derivatives at the boundaries between regions. We match the wave functions from regions *I* and *II* at the boundary, i.e., ($x = 1/2$, $0 \leq y \leq R$). The wave function in region *I* has the form

$$\psi(x = 1/2, y) = \psi_I(x = 1/2, y) \quad (y \leq 1) = 0 \quad (R \geq y > 1). \quad (\text{A2})$$

We also equate the normal derivatives at the boundary, i.e., $(\partial\psi/\partial x)|_{x=1/2}$. Here the wave functions in the two regions are matched only over the interval $0 \leq y \leq 1$. The matching is carried out by expanding the wave functions in both regions in a complete orthogonal basis which vanishes on the boundary; for the wave function we expand both sides in terms of $\sin(n\pi y/R)$, and for the normal derivatives we expand both sides in $\sin(n\pi y)$.

The bound states are obtained by truncating the resulting expansions and solving the matrix equation. The condition for a bound state is $\text{Det}(\mathbf{Z}) = 0$, where $\mathbf{Z} = \mathbf{TS} - \mathbf{1}$, and

$$\begin{aligned} \mathbf{T}_{nk} &= -\frac{\beta_k}{\alpha_n} \exp(\alpha_n/2) u_{kn} \sinh(\beta_k/2) \quad (k \text{ odd}) \\ &= -\frac{\beta_k}{\alpha_n} \exp(\alpha_n/2) u_{kn} \cosh(\beta_k/2) \quad (k \text{ even}), \\ \mathbf{S}_{nk} &= \frac{u_{nk}}{R} \frac{\exp(-\alpha_k/2)}{\cosh(\beta_n/2)} \quad (n \text{ odd}) \\ &= \frac{u_{nk}}{R} \frac{\exp(-\alpha_k/2)}{\sinh(\beta_n/2)} \quad (n \text{ even}), \\ u_{nk} &= (-1)^{k+1} \frac{2k \sin(n\pi/R)}{\pi k^2 - n^2/R^2}. \end{aligned} \quad (\text{A3})$$

In this region the only bound states occur for wave functions symmetric under reflection. The bound state wave function has a single peak in the bend region. In Fig. 10, we plot the density contours for the bound state wave function for the case $R = 1.5$.

-
- ¹M.L. Roukes, A. Scherer, S.J. Allen, Jr., H.G. Craighead, R.M. Ruthern, E.D. Beebe, and J.P. Harbison, *Phys. Rev.* **59**, 3011 (1988).
- ²G. Timp, H.U. Baranger, P. deVegvar, J.E. Cunningham, R.E. Howard, R. Behringer, and P.M. Mankiewich, *Phys. Rev. Lett.* **60**, 2081 (1988).
- ³F.M. Peeters, *Superlatt. Microstruct.* **6**, 217 (1989).
- ⁴H.U. Baranger, A.D. Stone, and D.P. DiVincenzo, *Phys. Rev. B* **37**, 6521 (1988).
- ⁵Mark Reed, *Sci. Am.* **268**, 118 (1993).
- ⁶R.L. Schult, D.G. Ravenhall, and H.W. Wyld, *Phys. Rev. B* **39**, 5476 (1989).
- ⁷F. Lenz, J.T. Londergan, E.J. Moniz, R. Rosenfelder, M. Stingl, and K. Yazaki, *Ann. Phys. (N.Y.)* **170**, 65 (1986).
- ⁸J. Goldstone and R.L. Jaffe, *Phys. Rev. B* **45**, 14 100 (1992); G. Dunne and R.L. Jaffe, *Ann. Phys. (N.Y.)* **223**, 180 (1993).
- ⁹P. Exner and P. Seba, *J. Math. Phys.* **30**, 2574 (1989).
- ¹⁰P. Exner, *Phys. Lett. A* **141**, 213 (1989).
- ¹¹J. Carini, J.T. Londergan, Kieran Mullen, and D.P. Murdock, *Phys. Rev. B* **46**, 15 538 (1992).
- ¹²J. Carini, J.T. Londergan, Kieran Mullen, and D.P. Murdock, *Phys. Rev. B* **48**, 4503 (1993).
- ¹³See, e.g., L. Lewin, *Theory of Waveguides* (Newnes-Butterworth, London, 1975).
- ¹⁴J.C. Wu, M.N. Wybourne, W. Yindeepol, A. Weisshaar, and S.M. Goodnick, *Appl. Phys. Lett.* **59**, 102 (1991); W. Yindeepol, A. Chin, A. Weisshaar, S.M. Goodnick, J.C. Wu, and M.N. Wybourne, *Nanostructures and Mesoscopic Systems*, edited by W.P. Kirk and M.A. Reed (Academic Press, Boston, 1992), pp. 139–149.
- ¹⁵P.L. McEuen, B.W. Alphenaar, R.G. Wheeler, and R.N. Sacks, *Surf. Sci.* **229**, 312 (1990).
- ¹⁶C.-K. Wang, K.-F. Berggren, and Z.-L. Ji, *J. Appl. Phys.* **77**, 2564 (1995).
- ¹⁷C.-K. Wang, *Semicond. Sci. Technol.* **10**, 1131 (1995).
- ¹⁸John P. Carini, J.T. Londergan, and D.P. Murdock, following paper, *Phys. Rev. B* **55**, 9852 (1997).
- ¹⁹Y. Avishai, D. Bessis, B.G. Giraud, and G. Mantica, *Phys. Rev. B* **44**, 8028 (1991).
- ²⁰F. Sols and M. Macucci, *Phys. Rev. B* **41**, 11 887 (1990).
- ²¹K.-F. Berggren and Z.-L. Ji, *Phys. Rev. B* **43**, 4760 (1991); K.-F. Berggren, C. Besev, and Z.-L. Ji, *Phys. Scr.* **T42**, 1441 (1992); H. Xu, Z.-L. Ji, and K.-F. Berggren, *Superlatt. Microstruct.* **12**, 237 (1992); K.-F. Berggren and Z.-L. Ji, *Phys. Rev. B* **47**, 6390 (1993).
- ²²C.S. Lent, *Appl. Phys. Lett.* **57**, 1678 (1990); **56**, 2554 (1990); C.S. Lent and D.J. Kirkner, *J. Appl. Phys.* **67**, 6353 (1990).
- ²³L.C. Maier and J.C. Slater, *J. Appl. Phys.* **23**, 68 (1954); J.C. Amato and H. Herrmann, *Rev. Sci. Instrum.* **56**, 696 (1985).
- ²⁴S. Sridhar, *Phys. Rev. Lett.* **67**, 785 (1991); S. Sridhar and E.J. Heller, *Phys. Rev. A* **46**, R1728 (1992).